Conductivity at Low Humidity of Materials Derived from Ferroxane Particles

Lapina, Alberto; Holtappels, Peter; Mogensen, Mogens Bjerg

Published in:
International Journal of Electrochemistry

Link to article, DOI:
10.1155/2012/930537

Publication date:
2012

Document Version
Publisher's PDF, also known as Version of record

Hindawi Publishing Corporation
International Journal of Electrochemistry
Volume 2012, Article ID 930537, 7 pages
doi:10.1155/2012/930537

Research Article

Conductivity at Low Humidity of Materials Derived from Ferroxane Particles

Alberto Lapina, Peter Holtappels, and Mogens Mogensen

Department of Energy Conversion and Storage, Technical University of Denmark, Frederiksborgvej 399, P.O. Box 49, 4000 Roskilde, Denmark

Correspondence should be addressed to Alberto Lapina, alap@risoe.dtu.dk

Received 23 May 2012; Revised 4 October 2012; Accepted 9 October 2012

Academic Editor: Abel César Chialvo

Carboxylic-acid-stabilised γ-FeOOH particles (ferroxanes) are synthesized using a precipitation from aqueous solution, and a following reaction with acetic acid. The materials produced with these powders are investigated by XRD, SEM, nitrogen adsorption-desorption, and impedance spectroscopy. Conductivity of both sintered and unsintered materials decreases strongly with a decrease in water partial pressure in the atmosphere during the test. The highest conductivity ($7 \cdot 10^{-3}$ S cm^{-1}) is measured in air ($p_{H_2O} = 0.037$ atm) at room temperature on sintered material. The conductivity values are compared with other works in the literature and the dependence of conductivity on surface area and pore size is discussed. It is suggested that both unsintered and sintered materials act as proton conductors at room temperature under moderate humidity conditions.

1. Introduction

There is nowadays a deep interest in the development of fuel cells and electrolyzers based on proton conducting electrolytes. Such devices span from proton exchange membrane fuel cells (PEMFCs) to proton conducting ceramic fuel cells (PCFCs). In all these cells the functional behavior of the electrolyte is strongly dependent on the humidity of the atmosphere in which it operates: in particular Nafion membranes used in PEMFCs require high relative humidity to retain high proton conductivity [1]. In order to simplify the fuel cell system it is convenient to use an electrolyte stable in low humidity conditions, and whose proton conductivity is independent of humidity. Moreover, some applications, such as electrochemical synthesis of ammonia [2, 3], could require the electrochemical system to work in low humidity conditions.

During the last decade materials derived from carboxylic-acid-stabilized γ-FeOOH nanoparticles (ferroxanes) have been investigated as proton conductors by Tsui et al. [4] Tsui and Wiesner [5], Rose et al. [6]. These studies report conductivities up to $2.65 \cdot 10^{-2}$ S cm^{-1} at room temperature [4] and for some of the materials investigated the conductivity is reported to be almost independent of the relative humidity in the range 30–100% at room temperature (equivalent to $p_{H_2O} = 0.0096$–0.032 atm). These materials are therefore interesting candidates as proton conducting electrolytes.

The model proposed for the conduction mechanism [4, 7] suggests two main mechanisms for proton conduction, both at the surface of the material: conduction by hydroxyl groups in a chemisorbed water layer and conduction in a physisorbed water layer.

In low humidity conditions, the physisorbed layer is absent and only a chemisorbed layer (that gets formed on first contact with water vapor) is present; this layer is reported not to be affected by changes in humidity, but to be removable if the temperature is increased [4]. The conduction takes place by proton hopping between the hydroxyl groups.

At higher humidity layers of physisorbed water cover the surface and protons combine with water molecules forming H_3O^+ then hop to the neighbor water molecules in the layer: this process is known as Grotthuss chain reaction [4].

In a recent work Guo and Barnard [8] studied by DFT calculations the possibility of having proton transfer between OH groups on the side of the Fe octahedra sheets in the layered structure of lepidocrocite (γ-FeOOH). Such

a process is reported to have a moderate energy barrier and is theoretically independent of the hydration conditions. However, the conductivity of the material is expected to be extremely anisotropic since the proton conduction takes place only parallel to the layers.

In this paper we measure the conductivity of unsintered and sintered material produced from ferroxanes powders. We study it in a range of low humidities at 25°C and 40°C.

2. Experimental

2.1. Synthesis. The lepidocrocite (γ-FeOOH) and ferroxane powders are prepared by a synthesis procedure based on what is reported in the literature [4, 6, 7]. The synthesis procedure is shown in Figure 1 and described hereunder.

A NaOH aqueous solution (0.2 M) is added to a $FeCl_2 \cdot 4H_2O$ solution (0.12 M) under stirring, keeping a ratio $[FeCl_2 \cdot 4H_2O]/[NaOH] = 0.6$, which is reported to favor the formation of pure lepidocrocite [6, 9]. This produces a suspension having a dark green colour, which is stirred at room temperature for 12–20 hours, until it turns orange in colour. The suspension is centrifugated for 1-2 hours at 4000 rpm (Sigma 2–16 centrifuge) to separate the lepidocrocite particles from the liquid and the NaCl contained in it. The lepidocrocite particles obtained by centrifugation are dried at 90°C and then dissolved again in distilled water, together with pure acetic acid (CH_3COOH), keeping a ratio [Fe/AA] = 1.5. The dispersion is again stirred at room temperature for 12–20 hours and centrifugated for 1-2 hours at 4000 rpm. The reactions taking place have been described by Rose et al. [6].

The obtained ferroxane powders are dried at 90°C, manually grounded and pressed into pellets (diameter 8 mm, thickness 0.9–1.2 mm) by uniaxial pressing (600 GPa). While half of the pellets are not sintered (i.e., "green" pellets), half of them undergo sintering in air (4 hours at 300°C or 500°C, 1°C/min heating and cooling rates).

XRD analysis of powders and both green and sintered pellets is carried out using a STOE X-ray diffractometer (Cu K-α radiation, acceleration voltage 40 kV, filament current 30 mA). The materials are imaged with a scanning electron microscope (Zeiss SUPRA SEM). The samples are attached to a metal sample holder using carbon tape and coated with a thin layer of carbon using a sputter coater.

2.2. Nitrogen Adsorption-Desorption. Surface area and pore size distribution are measured by nitrogen adsorption-desorption using an Authosorb-1MP instrument (Quantachrome Instruments, Germany). Manually grinded samples are degassed at 120°C for 10 hours prior to adsorption/desorption. Samples of circa 0.1 g are measured using nitrogen as adsorbate gas. The isotherms obtained are used to calculate the surface area and the pore size distribution.

2.3. Electrochemical Testing. Both unsintered (green) and sintered pellets are tested, using the same electrodes on both faces of each pellet. Two different kinds of electrodes are used. Disks of carbon paper loaded with Pt nanoparticles (IRD Fuel Cells, Denmark) are put in contact with both the faces of the pellet to act as electrodes. Gold electrodes (about 500 nm thick) are deposited by plasma sputtering with a deposition rate of 27 nm/min. The electrical connections to the electrodes are ensured by pressing a Pt mesh on them.

Electrochemical measurements are conducted at room temperature (24–30°C) or at 40°C, under a constant flow (50 mL/min) of air. The gas is either dry (i.e., nonhumidified, $p_{H_2O} \approx 0.001$ atm) or humidified by bubbling through a water bottle hold at 12°C ($p_{H_2O} = 0.014$ atm) or 28°C ($p_{H_2O} = 0.037$ atm). The measurements reported in this work are carried out once the system has reached equilibrium: depending on the parameter changed (temperature, p_{H_2O}), up to 50 hours can be necessary to reach it.

Two-point impedance spectroscopy is performed using a Solartron 1260 Frequency Response Analyzer (Solartron Analytical, UK). Impedance spectra are recorded in the frequency range 980 kHz–1.23 Hz applying a sinusoidal signal with an amplitude of 0.2 V and are analyzed with commercial softwares ZView (Scribner Associates, USA) and ZSimpWin (EChem Software, USA).

The conductivity σ of the material is calculated with the following equation:

$$\sigma = \frac{t}{R \cdot A}, \tag{1}$$

where t is the thickness of the tested pellet, A is the area of the cross section of the pellet (0.5 cm^2), and R is the electrolyte resistance.

3. Results

3.1. X-Ray Diffractometry. The XRD patterns for lepidocrocite particles and ferroxane particles, that is, before and after exposure to acetic acid, are reported in Figure 2. In both cases the only phase detected is lepidocrocite (γ-FeOOH, PDF number 0044–1415), proving that the crystallographic structure of the powders remains unchanged upon exposure to acetic acid.

Sintering at 300°C induces a phase transformation in the material, which becomes maghemite (γ-Fe_2O_3, PDF number 0025–1402), as shown in Figure 3(a): the peak at $2\theta = 44.2°$ is due to the sample holder.

Since in this study we are interested in making a comparison with the studies carried out by other groups on hematite [4, 10, 11], we sinter the material at higher temperature to obtain hematite. According to DTA measurements by Ye et al. [12] the phase transition temperature between nanocrystalline maghemite and hematite is between 440°C and 550°C. In our work sintering at 500°C gives single-phase hematite (α-Fe_2O_3, PDF number 033–0664), as shown in Figure 3(b).

3.2. Nitrogen Adsorption-Desorption. The ferroxanes, maghemite, and hematite powders have surface areas of 55 m^2/g, 103 m^2/g, and 22 m^2/g, respectively. The surface area doubles upon sintering at 300°C, but decreases dramatically if the sintering is carried out at 500°C.

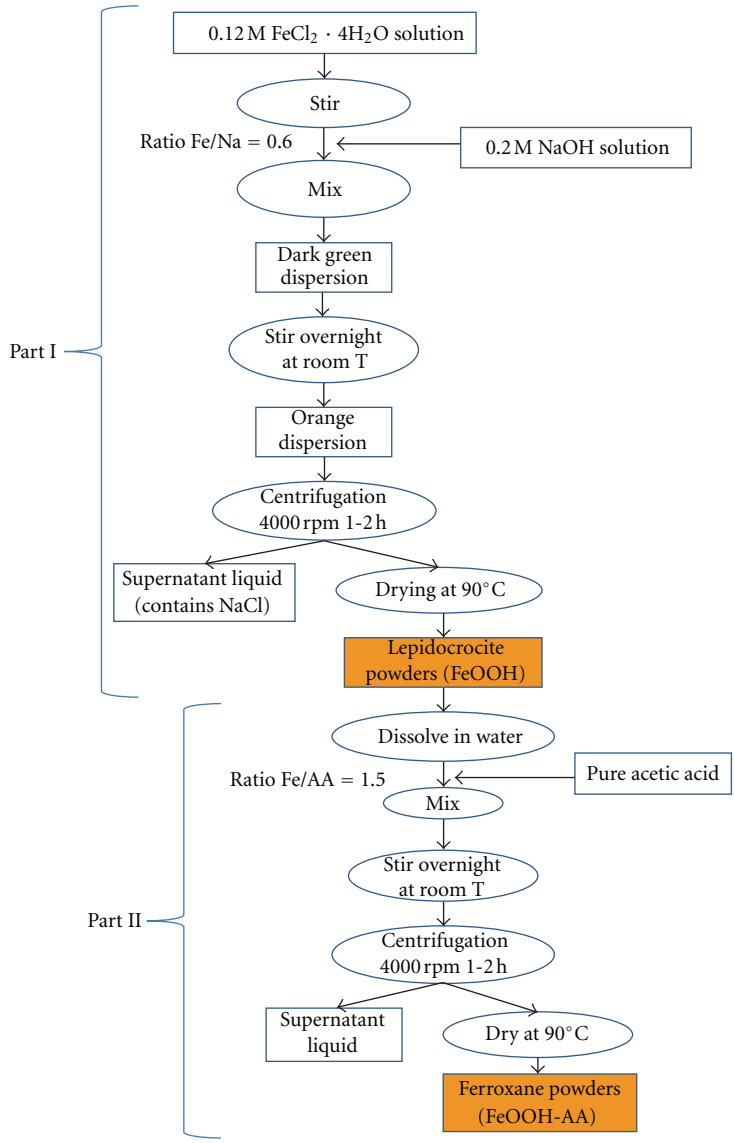

Figure 1: Flow chart for the ferroxane powders synthesis procedure.

Pore size distribution measurements show that all the powders have a very large average pore size, above 200 nm. Pores with size in the 2–20 nm range are present in the ferroxanes particles and in greater quantity in the maghemite particles, but they are absent in the hematite particles.

3.3. SEM Imaging. A SEM image of the ferroxanes powder is reported in Figure 4: the particles have an elongated shape, with a length of about 300 nm an a width of 100–150 nm, and exhibit significant agglomeration. The cross sections of a green pellet (i.e., produced pressing the powders shown in Figure 4) and of a pellet sintered at 300°C are shown in Figure 5.

3.4. Electrochemical Testing. To describe the impedance spectra measured at moderate humidity we propose the equivalent circuit $R(C(R_1(WR_W)))(R_{el}Q_{el})$, presented in Figure 6 together with an example of impedance spectrum.

In this circuit C is assumed to be the geometrical capacitance of the system, W the infinite Warburg impedance element describing the diffusion of charge carriers in the water in the pores of the material, R_W the resistance to the charge carriers movement along the physisorbed/chemisorbed layer of water on the particles, and R_{el} and Q_{el}, respectively, the resistance and the constant phase element associated with the electrode process [13]. Such a model, with two conduction mechanisms and an additional electrode mechanism, is in general agreement with the conduction mechanisms proposed so far for these materials. At higher humidities the resistance of the electrolyte processes decreases significantly and the impedance spectrum is dominated by the electrode contribution. At low humidity instead the electrolyte resistance increases and only one electrolyte process can be

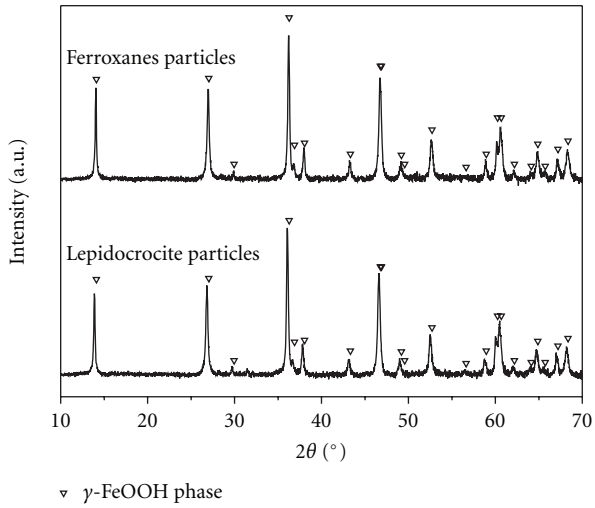

Figure 2: XRD diffractograms of lepidocrocite particles and ferroxane particles. The identical patterns show that the crystallographic structure of the powders remains unchanged upon exposure to acetic acid.

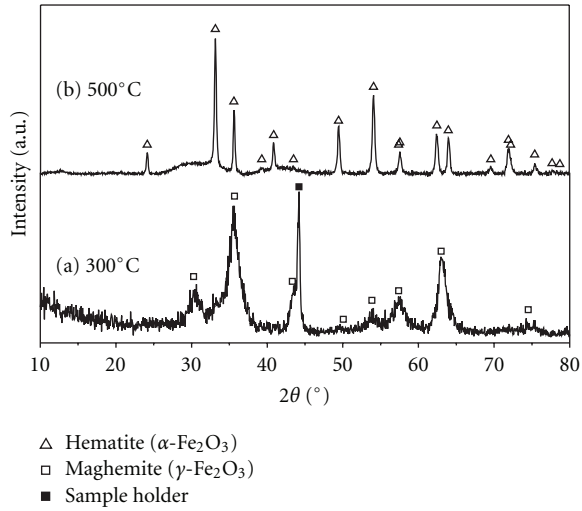

Figure 3: XRD diffractograms of pellets sintered for 4 hours at: (a) 300°C, (b) 500°C. The peak at $2\theta = 44.2°$ is due to the sample holder.

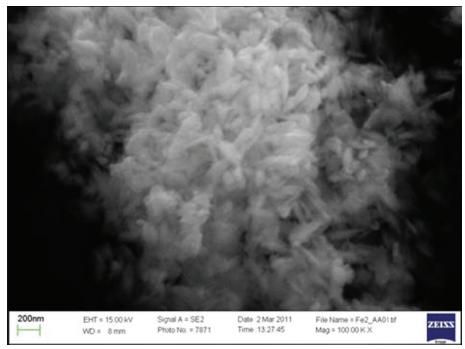

Figure 4: SEM image of ferroxane particles.

identified in the spectrum, while the electrode response is negligible.

The present data do not permit a deeper evaluation of the single contributions to the impedance of the material, therefore in the following only the total resistance of the electrolyte is considered to calculate its conductivity.

Conductivity versus p_{H_2O} at room temperature and at 40°C is reported in Figures 7 and 8, respectively. At both temperatures the conductivity of all the materials decreases orders of magnitude upon reducing water partial pressure. At $p_{H_2O} = 0.037$ atm green material and material sintered at 300°C (maghemite) have about the same conductivity, while it is about one order of magnitude lower for the material sintered at 500°C (hematite). At lower humidities the material sintered at 300°C shows the highest conductivity: this is particularly evident in Figure 8. The general trend in conductivity at low humidities is $\sigma_{300°C} > \sigma_{green} > \sigma_{500°C}$. The conductivity of the material sintered at 500°C at $p_{H_2O} = 0.001$ atm is not reported in Figures 7 and 8 because it is too low to be measured.

Concerning the effect of temperature, a comparison of Figures 7 and 8 shows that conductivities measured at $p_{H_2O} = 0.037$ atm are significantly lower at 40°C than at room temperature.

4. Discussion

4.1. Crystallographic Structure. The powders have the crystallographic structure of lepidocrocite (γ-FeOOH) both before and after the treatment with acetic acid, which is consistent with previous literature reports [6]. After sintering at 300°C maghemite (γ-Fe_2O_3) is obtained instead of hematite (α-Fe_2O_3) as reported by Rose et al. [6]. In this work, sintering at 500°C was necessary to obtain pure hematite.

In the present work the ferroxane powders are used to fabricate pellets by uniaxial pressing, while other authors fabricate unsupported [4, 5] and glass fibers supported [14] membranes by drying a suspension of particles. The green pellets and the hematite pellets in this work have therefore the same crystallographic structure as the material reported in other works, but the microstructure is different because of the different fabrication procedure. A nonpressed thin membrane is expected to have a lower density than our material.

4.2. Conductivity. The conductivity of the green material presented in this work shows the same trend versus humidity as the one presented by Tsui et al. [4], but with values 1-2 orders of magnitude lower. Also the sintered materials show a decrease in conductivity with a decrease in humidity, while Tsui et al. [4] report almost constant conductivities down to 30% relative humidity.

Such differences can be explained taking into account the surface area and the pore size of the particles in the two studies. The values of surface areas in this work are quite similar to the ones reported by Tsui and follow the same trend: sintering at 300°C increases surface area, while sintering at higher temperatures causes a decrease. On the

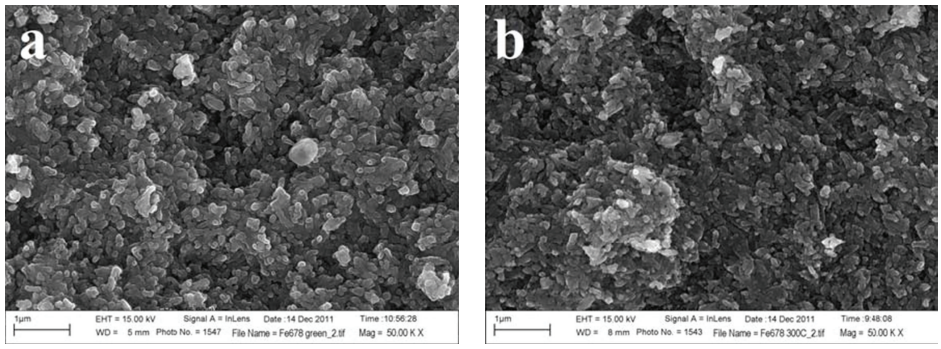

Figure 5: SEM image of a cross section (fracture) of (a) green pellet and (b) pellet sintered at 300°C, both not tested electrochemically.

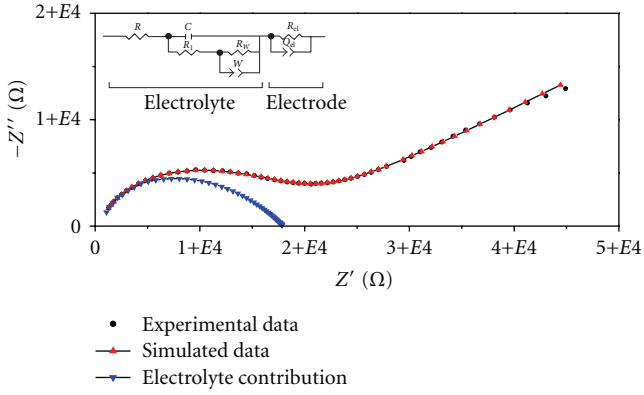

Figure 6: Nyquist plot for material sintered at 300°C and tested at 40°C in air, $p_{H_2O} = 0.037$ atm, using C-Pt electrodes. The "simulated data" curve shows the results of the fitting using the equivalent circuit represented, while the "electrolyte contribution" curve shows the contribution of the first part of the circuit.

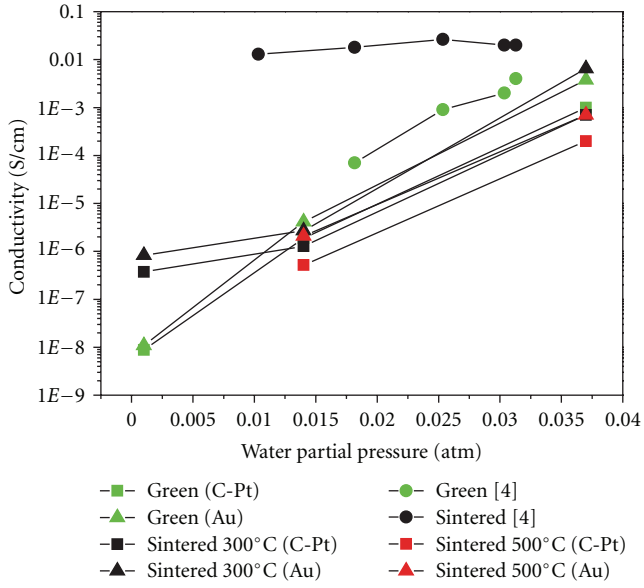

Figure 7: Conductivity versus water partial pressure, for materials tested in air at room temperature.

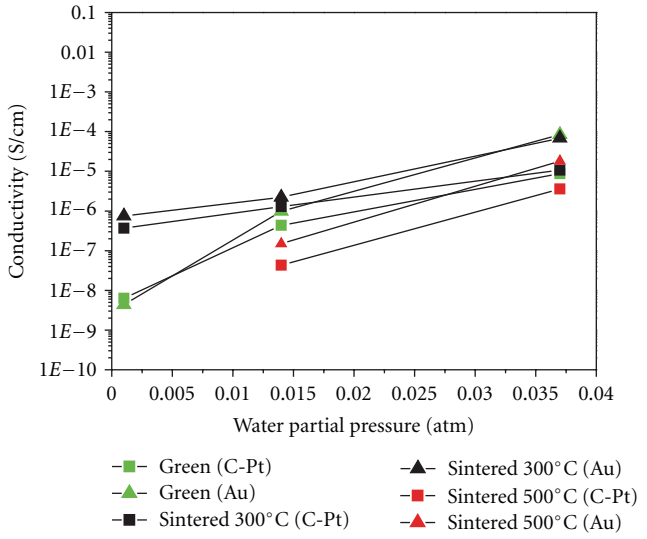

Figure 8: Conductivity versus water partial pressure, for materials tested in air at 40°C.

contrary, the average pore size is very different: while it is above 200 nm in the present work for all the powders, Tsui reports values in the 10–40 nm range.

These results support the hypothesis, suggested by Colomer and Anderson [15], that the effect of pore size on the proton conductivity is more important than the effect of the surface area.

It has been suggested [4] that both macroporosity (pore sizes > 50 nm) and microporosity (pore sizes < 2 nm) can be detrimental to proton conductivity, while a mesoporous structure (2 nm < pore sizes < 50 nm) is the best option to maximize the proton conductivity of iron oxide membranes. Hereunder we compare our results with other works reporting different surface areas and pore sizes to gather evidence to support this hypothesis.

Colomer and Zenzinger [10] studied hematite membranes having high surface areas (130–240 m^2/g) but very small average pore size (2–4 nm) and conductivities of about 10^{-6}–10^{-7} S/cm at 30% relative humidity (circa $p_{H_2O} = 0.01$ atm). Water uptake studies show that the surface of the material adsorbs or desorbs water depending on the

relative humidity of the environment, and the conductivity of the materials decreases with decreasing relative humidity. The temperature dependence of the conductivity (measured at constant relative humidity) suggests that the protons migrate by Grotthuss mechanism. The low values of proton conductivity are probably due to changes in proton mobility and concentration due to structure of pore water [16], which depends on the material and on the size of the pores. In very small pores it is likely that a higher fraction of the water in the pore is affected by the pore wall (the average pore in these materials has a diameter only about 10 times the diameter of a water molecule).

If instead the average pore size is two orders of magnitude larger (pore size > 200 nm), as in our work, at high humidities the pores are filled by physisorbed layers of water, but at lower humidities the physisorbed water is not retained by the structure and conductivity decreases dramatically. Also upon heating at 40°C with $p_{H_2O} = 0.037$ atm the physisorbed water in the large pores is partially removed and thus the conductivity decreases 1-2 orders of magnitude. The values of conductivity are of the same order of magnitude as the ones presented by Colomer and Zenzinger [10].

The sintered materials produced by Tsui et al. [4], having an average pore size of 10–40 nm, exhibit instead much higher conductivities ($\approx 10^{-2}$ S/cm) than the materials with pores one order of magnitude bigger or smaller in size. The fact that the conductivity of the sintered material only slightly decreases in the range 30–100% relative humidity suggests that physisorbed water is immobilized in the mesopores of the material and retained by the material at least down to 30% relative humidity.

So far we have shown how the overall conductivity values of our oxide materials (ferroxanes, maghemite, and hematite) fit into the general picture of the data available in literature. However, there are significant differences in conductivity among them, in particular in the very low humidity region (that has not been investigated by others so far) and in our opinion also these aspects can be explained taking into account the surface area and pore size data.

In general, the material sintered at 300°C exhibits the highest conductivity at all humidity values, both at 25°C and 40°C. At $p_{H_2O} = 0.014$ atm and $p_{H_2O} = 0.037$ atm the green material has slightly lower conductivity values, and the material sintered at 500°C has values one order of magnitude lower. Higher values of surface area correspond to higher proton conductivities.

On top of that, there is a difference in pore size distribution among the materials. While all of them have average pore sizes above 200 nm the material sintered at 300°C has a small amount of porosity in the 2–20 nm pore size range, and the green material has a slightly smaller amount. Porosity of this size is instead totally absent in the material sintered at 500°C.

This small amount of mesoporosity could account for the very strong difference in conductivity among the three materials at $p_{H_2O} = 0.001$ atm, in particular the extremely low conductivity of the material sintered at 500°C. While the water in macropores totally desorbs in these conditions, mesopores would be able to retain some of the water and thus ensure a conduction path for the protons. Tsui et al. [4] report that a chemisorbed layer of water gets formed on the oxide materials upon exposure to water vapor and that such a layer cannot be removed exposing the material to a dry atmosphere. Our very low conductivity values at $p_{H_2O} = 0.001$ atm show that either the contribution of the chemisorbed layer to the proton conductivity is very low or that this layer is removed by continuously flushing the material with dry gas.

The same authors explain the lower conductivity of the green material compared to the sintered one suggesting that the carboxylic groups present at the surface of the particles (introduced by the reaction between lepidocrocite and acetic acid during the synthesis) hinder the mobility of the protons within the hydroxyl groups [4, 7]. Since the carboxylic groups are removed upon sintering, their hindering effect would affect only the green material. However, this mechanism would not explain the much lower conductivity of the material sintered at 500°C. Moreover, the presence of carboxylic groups could at the same time hinder the proton conductivity but also improve the adsorption of water, because of the higher acidity of the carboxylic group compared to the hydroxyl group. In general, it is likely that the effect of the presence of carboxylic groups at the surface on the proton conductivity is dependent on the size of the pores where the adsorption takes place.

An additional conduction mechanism has been suggested for lepidocrocite by Guo and Barnard [8], based on computational studies. The proton transfer would occur between OH groups on the side of the Fe octahedra sheets in the layered structure of lepidocrocite. Such a process is theoretically independent of the hydration conditions, therefore might be of interest in low-humidity conditions. However, it would take place only parallel to the layers forming the lepidocrocite structure, thus causing the protonic conductivity of the material to be highly anisotropic. Our materials are fabricated pressing randomly oriented lepidocrocite particles, thus only a fraction of them is expected to be oriented perpendicular to the electrodes during the test. Any contribution of this process to the total proton conductivity would be extremely low.

5. Conclusions

Ferroxane powders are synthesized using a precipitation from aqueous solution, and a following reaction with acetic acid. The materials produced with these powders are electrochemically tested in the lowest humidity conditions reported so far in the literature.

Both green and sintered materials exhibit a strong dependence of conductivity on humidity, which we attribute to the presence of macropores (>200 nm) that do not hinder water desorption. The analysis of presented data and the comparison with previous literature reports suggests that surface area and in particular pore size are the factors determining the proton conductivity of iron oxides materials. The very low conductivity values measured at $p_{H_2O} = 0.001$ atm suggest that either the chemisorbed water layer has a very low

proton conductivity or it is removed by exposing the material to dry gas.

Heating up the material from room temperature to 40°C causes a reduction of conductivity at high humidity values, likely due to the desorption of physisorbed water from the macropores.

The materials have relatively high conductivity (up to $7 \cdot 10^{-3}\,\mathrm{S\,cm^{-1}}$) and could be applied as proton conductor for room temperature, moderate humidity applications. Tailoring of the pore size to obtain mesoporosity is expected to improve the proton conductivity of the material at low humidities.

Acknowledgments

The authors thank Dr. Eugen Stamate for preparing the sputtered gold electrodes. This work was carried out within the Catalysis for Sustainable Energy Initiative, funded by the Danish Ministry of Science, Technology and Innovation.

References

[1] Y. Sone, P. Ekdunge, and D. Simonsson, "Proton conductivity of nafion 117 as measured by a four-electrode AC impedance method," *Journal of the Electrochemical Society*, vol. 143, no. 4, pp. 1254–1259, 1996.

[2] I. A. Amar, R. Lan, C. T. G. Petit, and S. Tao, "Solid-state electrochemical synthesis of ammonia: a review," *Journal of Solid State Electrochemistry*, vol. 15, pp. 1845–1860, 2011.

[3] A. Hellman, E. J. Baerends, M. Biczysko et al., "Predicting catalysis: understanding ammonia synthesis from first-principles calculations," *Journal of Physical Chemistry B*, vol. 110, no. 36, pp. 17719–17735, 2006.

[4] E. M. Tsui, M. M. Cortalezzi, and M. R. Wiesner, "Proton conductivity and methanol rejection by ceramic membranes derived from ferroxane and alumoxane precursors," *Journal of Membrane Science*, vol. 306, no. 1-2, pp. 8–15, 2007.

[5] E. M. Tsui and M. R. Wiesner, "Fast proton-conducting ceramic membranes derived from ferroxane nanoparticle-precursors as fuel cell electrolytes," *Journal of Membrane Science*, vol. 318, no. 1-2, pp. 79–83, 2008.

[6] J. Rose, M. M. Cortalezzi-Fidalgo, S. Moustier et al., "Synthesis and characterization of carboxylate–FeOOH nanoparticles (ferroxanes) and ferroxane-derived ceramics," *Chemistry of Materials*, vol. 14, no. 2, pp. 621–628, 2002.

[7] L. Zhang, *Synthesis and characterization of novel proton-conductive composite membranes derived from the hybridization of metal oxyhydroxide nanoparticles and organic polymers for fuel cell applications [M.S. thesis]*, Duke University, 2010.

[8] H. Guo and A. S. Barnard, "Proton transfer in the hydrogen-bonded chains of lepidocrocite: a computational study," *Physical Chemistry Chemical Physics*, vol. 13, no. 39, pp. 17864–17869, 2011.

[9] P. Refait and J. M. R. Génin, "The oxidation of ferrous hydroxide in chloride-containing aqueous media and pourbaix diagrams of green rust one," *Corrosion Science*, vol. 34, no. 5, pp. 797–819, 1993.

[10] M. T. Colomer and K. Zenzinger, "Mesoporous α-Fe_2O_3 membranes as proton conductors: synthesis by microwave-assisted solgel route and effect of their textural characteristics on water uptake and proton conductivity," *Microporous and Mesoporous Materials*, vol. 161, pp. 123–133, 2012.

[11] M. T. Colomer, "Proton transport, water uptake and hydrogen permeability of nanoporous hematite ceramic membranes," *Journal of Power Sources*, vol. 196, no. 20, pp. 8280–8285, 2011.

[12] X. Ye, D. Lin, Z. Jiao, and L. Zhang, "The thermal stability of nanocrystalline maghemite Fe_2O_3," *Journal of Physics D*, vol. 31, no. 20, pp. 2739–2744, 1998.

[13] E. Barsoukov and J. R. Macdonald, *Impedance Spectroscopy: Theory, Experiment, and Applications*, Wiley-Interscience, 2005.

[14] M. M. Cortalezzi, J. Rose, G. F. Wells, J. Y. Bottero, A. R. Barron, and M. R. Wiesner, "Ceramic membranes derived from ferroxane nanoparticles: a new route for the fabrication of iron oxide ultrafiltration membranes," *Journal of Membrane Science*, vol. 227, no. 1-2, pp. 207–217, 2003.

[15] M. T. Colomer and M. A. Anderson, "High porosity silica xerogels prepared by a particulate sol-gel route: pore structure and proton conductivity," *Journal of Non-Crystalline Solids*, vol. 290, no. 2-3, pp. 93–104, 2001.

[16] P. Colomban, *Proton Conductors: Solids, Membranes and Gels—Materials and Devices. Chemistry of Solid State Materials*, Cambridge University Press, 1992.